Available online at www.sciencedirect.com
SCIENCE DIRECT®
Journal of Magnetic Resonance 165 (2003) 248–252
JMR Journal of Magnetic Resonance
www.elsevier.com/locate/jmr

A high sensitivity 3D experiment for measuring C_α–H_α residual dipolar coupling constants

Weidong Hu,* Ziming Zhang, and Yuan Chen

Division of Immunology, Beckman Institute of the City of Hope, Duarte, CA 91010, USA

Received 12 July 2003; revised 20 August 2003

Abstract

A new sensitivity improved approach is presented to measure the C_α–H_α scalar and dipolar coupling constants in $^{13}C/^{15}N$-labeled proteins using a HA(CA)CONH scheme. The proposed experiment has significantly higher sensitivity than the previously published (HA)CA(CO)NH sequence, and provides accurate and straightforward measurements of the scalar and residual dipolar coupling constants. The sequence is easy to implement, and has been demonstrated on the C-terminal domain of the human Ku-80 protein (152 amino acid residues). On average, sensitivity is improved by 40% for both isotropic and anisotropic samples. The sensitivity enhancement is more pronounced for structured regions than unstructured regions, with an average of 50–60% enhancement being observed in the well-structured regions of the protein.

Keywords: HA(CA)CONH; Scalar couplings; Dipolar couplings; Protein; Solution NMR

1. Introduction

Residual dipolar coupling constants have been used successfully in structural determination of macromolecules by solution NMR methods [1,2]. Dipolar coupling constants provide information on the orientation of the bond vectors with respect to the anisotropic alignment tensor of the molecule. Thus, dipolar coupling constants provide long-range structural information that complements the distance and torsional angle restraints derived from NOE and scalar coupling constants. The most common dipolar coupling constants measured in protein samples are those associated with the one-bond amide N–H, C_α–H_α, C'–C_α and C'–N groups. These dipolar couplings have been used in structural refinements [3], in obtaining protein folds and determining structures de novo [4–6], in structural quality evaluation [7], and in docking protein–protein complexes [8]. The dipolar couplings can be obtained from measuring the difference between the couplings measured from the sample in isotropic and anisotropic phases [2,9]. Methodology development for the measurement of residual dipolar coupling constants in macromolecular systems is strongly motivated by these promising applications.

The amide N–H and the C_α–H_α coupling constants can be obtained with high accuracy relative to other one-bond couplings involving backbone atoms, as these two inter-nuclear vectors have the largest dipolar coupling interactions among the backbone vectors in a protein. These large interactions are due to the large ^1H gyromagnetic ratio and the short bond distances between these atom pairs. Because of their large values and higher accuracies, the N–H and C_α–H_α residual dipolar coupling constants are the most frequently used in the application of dipolar coupling restraints.

Several methods have been developed for the measurement of the C_α–H_α coupling constants. It's measurement can be proceeded in a quantitative *J*-correlation manner, either from a 2D correlation of ^{13}C–^1H using constant-time HSQC [10] or from a 2D correlation of ^{15}N–^1H using a (HACACO)NH sequence [11]. Although the later approach offers better resonance dispersion, resonance degeneracy occurs in these 2D methods, especially for large proteins. To reduce the resonance overlap, several 3D triple-resonance

* Corresponding author. Fax: 1-626-301-8186.
E-mail address: whu@coh.org (W. Hu).

1090-7807/$ - see front matter © 2003 Elsevier Inc. All rights reserved.
doi:10.1016/j.jmr.2003.08.008

experiments have been proposed to measure the C_α–H_α coupling constant. In one HNCO-based experimental approach, the coupling of C_α–H_α is embedded in the C' dimension, and resonance overlap is further reduced by separating the two coupling components into two subspectra [12]. The drawback of the sequence, as pointed out by Rule and co-workers [11], is that the active C_α–C_β coupling causes an under-digitization in the coupling (C_α–H_α) detection dimension, and may thus compromise the accuracy of the measurement. More recently, Bax and co-workers have proposed a quantitative measurement for C–H dipolar coupling constants using a CB(CA)CONH experiments [13]. This approach offers relatively high sensitivity and can be used to obtain couplings of both C_α–H_α and C_β–H_β. However, six 3D experiments are needed in order to extract the dipolar coupling of C_α–H_α, thus requiring an extensive period of instruments time to complete the measurement. Alternatively, the C_α–H_α can be measured in the (HA)CA(CO)NH sequence [14], in which the C_α–H_α dipolar coupling is active during the constant-time period for chemical shift labeling of C_α [15,16]. The constant-time period is set to $1/J_{C\alpha-C\beta}$, a compromised duration to allow both sufficient digital resolution for measuring the C_α–H_α coupling constants and to minimize the signal loss due to C_α–C_β coupling. Since the two components of C_α–H_α couplings are well resolved, two experiments (one in isotropic and the other in anisotropic media) are usually sufficient to extract the residual dipolar coupling constants for a medium-size protein. An IPAP scheme [17] can be added to resolve overlaps in the C_α region if needed. A major drawback to use (HA)CA(CO)NH experiment to measure the C_α–H_α coupling constant is that significant signal loss occurs during the long period of constant-time caused by the fast T_2 relaxation of C_α. The sensitivity of an

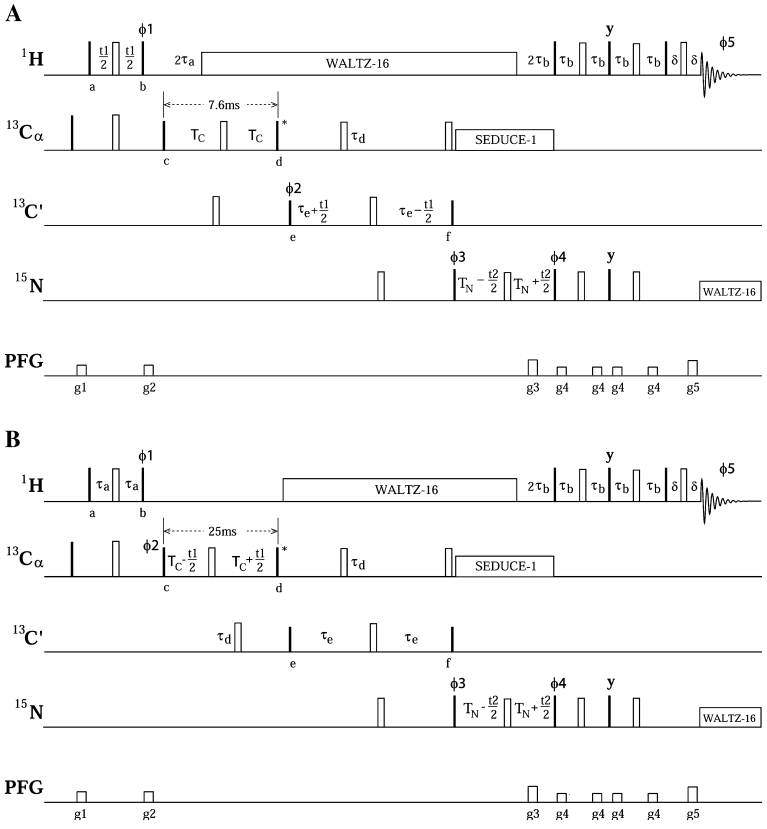

Fig. 1. Pulse schemes of 3D-HA(CA)CONH (A) and (HA)CA(CO)NH (B) experiments for measuring coupling constants of C_α–H_α. Narrow and wide bars represent 90° and 180° pulses, respectively. All pulses are along x-axis unless indicated otherwise. The ^1H and ^{15}N carrier frequencies are at 4.77 and 118 ppm. The ^{13}C carrier frequency was set initially at 55 ppm and then moved to 176 ppm after the first two high power pulses on C_α. Field strengths of the ^1H and ^{15}N pulses are 36 and 9.3 kHz. The power of decoupling WALTZ16 pulse [21] on ^1H and ^{15}N are 7.2 and 1.3 kHz, the power of decoupling SEDUCE-1 pulse [22] on $^{13}C_\alpha$ is 0.83 kHz. The durations of 90° and 180° pulses on C_α after the first two pulses are 64 and 57 μs so that they do not disturb the C' region. The same durations were also used for C' 90° and 180° pulses. The 90° pulse on C_α labeled with "*" has phase adjustment to correct the Bloch–Siegert shift caused by the 180° pulse on C'. Strengths and duration of gradients are $g1 = g2 = (22.5\,G/cm, 0.5\,ms)$, $g3 = (33.75\,G/cm, 1.25\,ms)$, $g4 = (18\,G/cm, 0.5\,ms)$, $g5 = (32.56\,G/cm, 0.125\,ms)$. The durations are $\tau_a = 1.8$ ms, $\tau_b = 2.35$ ms, $\tau_d = 4.5$ ms, $\tau_e = 14$ ms and $T_N = 14$ ms. T_C is 3.8 ms for (A) and 12.5 ms for (B). Phase cycling are $\phi1 = y, -y$; $\phi2 = y, y, -y, -y$; $\phi3 = 4(x), 4(-x)$; $\phi4 = x$ and Acq. $(\phi5) = x, -x, -x, x, -x, x, x, -x$. Rance-Kay sensitivity enhancement scheme [23] was used on ^{15}N dimension, and the quadrature detection was achieved by alternating $\phi4$ between x and $-x$ in concert with the sign inversion of g3. For each complex point of ^{15}N dimension, the 180° phase was added to both $\phi3$ and $\phi5$. Quadrature detection for t1 was achieved via States-TPPI [24] on $\phi2$.

experiment for measuring the C_α–H_α coupling constants is a critical factor for medium and large-sized protein samples because deuteration of protein [18], a common way to suppress the $C_\alpha T_2$ relaxation for large proteins, would not be useful in this case because H_α is required to measure the C_α–H_α coupling constants.

In this communication, we present an sensitivity-improved approach for measuring C_α–H_α coupling constants using the same magnetization transfer pathway as in the (HA)CA(CO)NH scheme but dictating the coupling interaction using H_α instead of C_α. The pulse sequence for the HA(CA)CONH experiment is illustrated in Fig. 1A. For comparison purposes, the recently published (HA)CA(CO)NH sequence [15,16] is shown in Fig. 1B. Details of the differences between the proposed real-time HA(CA)CONH and previously published constant-time (HA)CA(CO)NH sequences are as follows: (i) To avoid a long constant-time delay during which C_α T_2 relaxation occurs as well as limitations imposed by C_α–C_β coupling upon the constant-time duration in the (HA)CA(CO)NH experiment, C_α–H_α coupling detection is moved to the beginning period of the sequence (points a to b) during which magnetization of H_α is along the x–y plane. Thus, the C_α–H_α coupling constants are detected in a real-time manner rather than through a constant-time period. The INEPT period used to transfer the magnetization from H_α to C_α in the (HA)CA(CO)NH ($2\tau_a$ in Fig. 1B) is omitted. (ii) The H_α chemical shift is refocused by the 180° proton pulse in the middle of the t_1 period. The removal of cross correlation relaxation between H_α dipole and C_α CSA is accomplished by using the 180° pulse on C_α, which gives more uniform intensity for the two coupling components. (iii) From points c to d, the magnetization is further relayed to C' and the duration is 7.6 ms, which is an optimized value to reduce dephase of the coherence caused by passive C_α–C_β coupling and to maintain the transfer efficiency from C_α to C'. The duration of the same period (points c to d) is 25 ms in the (HA)CA(CO)NH sequence. This period is optimized to resolve the two components of C_α–H_α couplings and to minimize the signal loss due to C_α–C_β coupling. (iv) To take advantage of the favorable resonance dispersion of C' nucleus, the C_α–H_α coupling in the proposed HA(CA)CONH sequence is encoded in the C' chemical shift labeling period from points e to f. During the period from points e to f, antiphase term associated with C' to C_α is refocused and magnetization transfer from C' to ^{15}N takes place for both pulse sequences. The rest of pulse sequences in both schemes are the same and will not be discussed further.

This particular approach (Fig. 1A) has two advantages relative to the constant-time approach (Fig. 1B). First, the real time version can reduce signal loss due to the T_2 relaxation of C_α resonance during a long constant-time period. Second, measuring C_α–H_α coupling in H_α dimension can avoid C_α–C_β coupling interference.

To test the new pulse scheme, four 3D data sets were acquired using schemes of Figs. 1A and B on the ^{13}C/^{15}N-labeled Ku-80 C-terminal domain dissolved in an isotropic and anisotropic phases. The Ku-80 C-terminal domain, composed of 152 residues, interacts with DNA–protein kinase catalytic subunit during DNA double strand break repair in the non-homologous end-joining pathway [19]. The concentrations of isotropic and anisotropic samples were 1.2 and 0.6 mM in 100 mM phosphate buffer (pH 6.0). The anisotropic sample was prepared using Pf1 phage [9], with a phage concentration at about 20 mg/mL. Experimental conditions and data processing for isotropic and anisotropic samples were identical, and have been discussed in the caption to Fig. 2. Data were processed and analyzed using nmrPipe [20] and Felix (Accelrys Inc.).

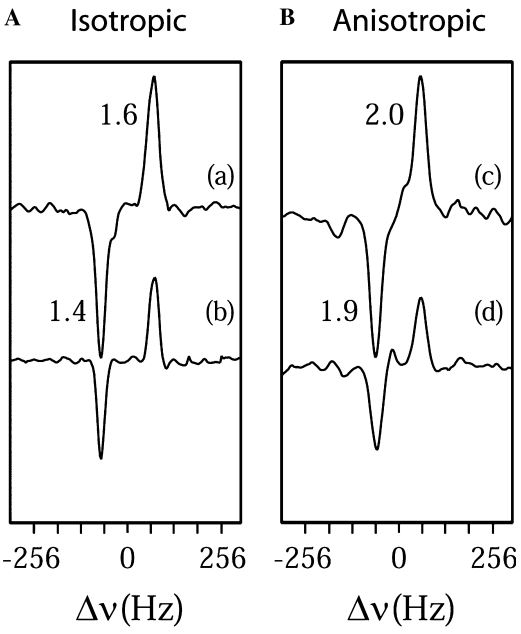

Fig. 2. Selected slices of spectra acquired using the HA(CA)CONH and (HA)CA(CO)NH experiments on isotropic (A) and anisotropic samples (B). The slices were extracted at $^1H = 7.68$ and $^{15}N = 119.3$ ppm, respectively. The slices of (a) and (c) are from the HA(CA)CONH experiment, and slices of (b) and (d) are from the (HA)CA(CO)NH experiment. The intensities of peaks from the HA(CA)CONH are significantly higher than those from the (HA)CA(CO)NH experiment, and the enhancement factors for both down-field and up-field components have been displayed in the Figure. The spectra were recorded with 24 scans per FID for isotropic sample, and 32 scans per FID for anisotropic sample. The total experimental time are 53 and 64 h for isotropic and anisotroipic samples, respectively. The spectra widths for F1/F2/F3 are 3268/1215.7/8000 Hz. The net acquisition times for F1/F2/F3 are 19.6/21.4/80 ms for isotropic and 18.4/21.4/80 ms for anisotropic samples, respectively. Both $t1$ and $t2$ time domains were apodized using cosine bell window function. The digital resolution in $F1$ was improved by zero-filling the $t1$ time domain to 256 prior to Fourier transformation. The data points of $t2$ time domain were doubled using mirror linear prediction [25], and zero-filled to 128 prior to transformation. The $t3$ domain was apodized using a 72° shifted sine bell window function and the data was zero-filled to 1024 points prior to transformation.

To illustrate the sensitivity difference between the two experiments, two slices along C' and C_α dimension at ^1H of 7.69 ppm and ^{15}N of 119.19 ppm are shown in Fig. 2. Slice (a) and (b) are from spectra recorded on an isotropic sample using the HA(CA)CONH and (HA)CA(CO)NH schemes, respectively. The peak intensities of the two couplings components in slice (a) are higher than those observed in slice (b). The enhancement factors for the up-field and down-field components are 1.6 and 1.4, respectively. Similar results have been observed for the oriented sample as shown in Fig. 2B in which slice (c) and (d) are from spectra obtained using the HA(CA)CONH and (HA)CA(CO)NH sequences, respectively. The sensitivity enhancement factors of slice (c) over slice (d) for up-field and down-field components are 2.0 and 1.9, respectively. To obtain a thorough comparison between the two pulse schemes, the intensities of all well-resolved peaks have been compared between spectra acquired using schemes HA(CA)CONH and (HA)CA(CO)NH on both isotropic and oriented samples. Extremely weak peaks, which came mostly from spectra recorded using the (HA)CA(CO)NH sequence, were excluded from the comparison. Gly residues were also not considered since their signals were suppressed significantly owing to the choice of the τ_a value in the HA(CA)CONH experiment. In all, 237 peaks (couplings components) have been compared for the spectra recorded on the isotropic sample. On average, the HA(CA)CONH scheme provided a factor of 1.4 enhancement in sensitivity over the (HA)CA(CO)NH scheme. For the anisotropic sample, the average sensitivity enhancement is a factor of 1.4 for 224 peaks (coupling components). These results show that the sensitivity can be enhanced significantly by the new HA(CA)CONH scheme for the measurement of C_α–H_α coupling constants.

Furthermore, the sensitivity enhancement is more significant for residues in the structured region than in the unstructured region. To demonstrate this observation, the experimental intensity ratios of individual residues versus the amino acid sequence have been presented along with the ^1H–^{15}N NOE values in Fig. 3. The ratios in Figs. 3B and C have been obtained from the isotropic and anisotropic samples, respectively. The label of "+" and "o" correspond to the up- and down-field components of the C_α–H_α couplings. It is interesting to note that no sensitivity enhancement has been observed for the unstructured N- and C-termini. The average sensitivity ratio is 0.95 and 0.94 for 28 peaks from the spectra recorded on the isotropic and anisotropic samples, respectively. The NOE values of these two regions are very small or negative, which suggests that these two regions are very flexible. On the other hand, the sensitivity ratios in a long loop region between

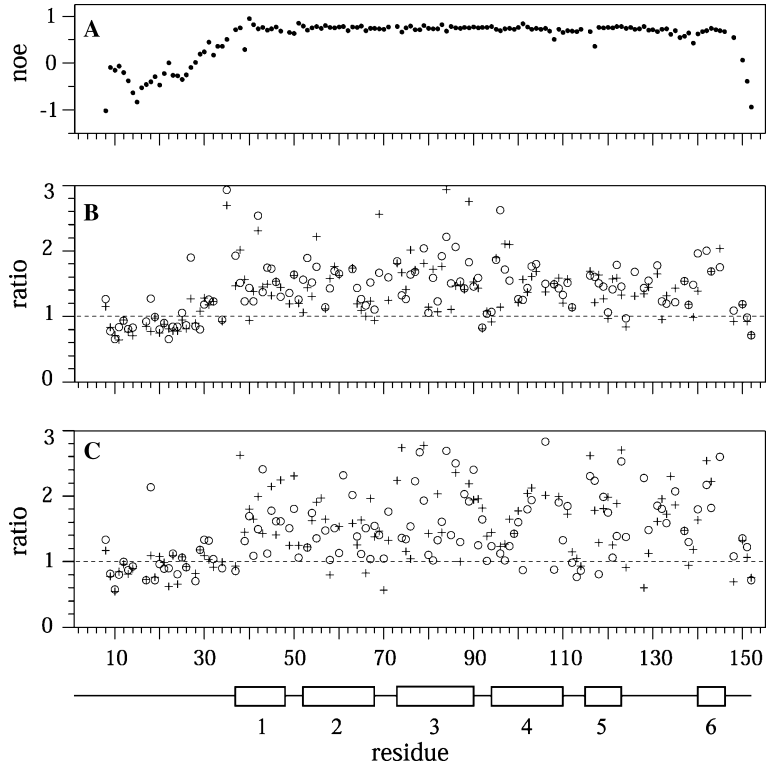

Fig. 3. Intensity ratios of individual coupling components from experiments of HA(CA)CONH and (HA)CA(CO)NH versus the primary sequence of Ku-80 DNA-binding domain. Shown together in panel (A) is the NOE of amide ^{15}N from amide proton. The Ku-80 DNA-binding domain is composed of six helices. The panel (B) and (C) are from isotropic and anisotropic samples, respectively. The label of "+" and "o" correspond to the up and down-field of the C_α–H_α coupling components.

helix 5 and 6, which has a normal ^{1}H–^{15}N NOE values, are approximately the same as those in regions of regular secondary structures. Thus, the enhancement for the well-ordered region of the protein is more pronounced. The absence of sensitivity improvements in the flexible region is consistent with the relative longer C_α T2 relaxation time of these residues compared to the residues in the rest of the protein, and this lack of sensitivity improvement is acceptable because the intrinsic peak intensity in flexible region is strong. Actually, when both the unstructured N- and C-termini are excluded from the comparison statistics, sensitivity enhancement factors of 1.5 (averaged over 181 peaks) and 1.6 (averaged over 168 peaks) have been obtained for isotropic and anisotropic samples, respectively. This observation suggests that the sensitivity improvement over the (HA)CA(CO)NH scheme should be more profound as the size of protein increases.

In summary, the proposed HA(CA)CONH approach offers a significantly improved sensitivity over (HA)CA(CO)NH sequence for measuring the C_α–H_α residual dipolar coupling constants. More importantly, sensitivity improvement is anticipated to be more pronounced as the protein size increases. This higher sensitivity makes this approach a valuable method for measuring C_α–H_α residual dipolar coupling constants. This sequence should be applicable to protein samples on which sufficient sensitivity can be achieved using the HA(CA)CONH experiment.

Acknowledgments

We appreciate that Dr. Rafael P. Brüschweiler kindly gave us Pf1 phage for our anisotropic sample preparation. We thank Drs. Ananya Majumdar and Aizhuo Liu for useful discussions. We thank Drs. Thomas A. Wilkinson and Mark Dizik for their critical reading and suggestions. This work is in part supported by NIH-CA94595 to Y.C.

References

[1] J.R. Tolman, J.M. Flanagan, M.A. Kennedy, J.H. Prestegard, Proc. Natl. Acad. Sci. USA 92 (1995) 9279–9283.
[2] N. Tjandra, A. Bax, Science 278 (1997) 1111–1114.
[3] N. Tjandra, J.G. Omichinski, A.M. Gronenborn, G.M. Clore, A. Bax, Nat. Struct. Biol. 4 (1997) 732–738.
[4] F. Delaglio, G. Kontaxis, A. Bax, J. Am. Chem. Soc. 122 (2000) 2142–2143.
[5] J.C. Hus, D. Marion, M. Blackledge, J. Mol. Biol. 298 (2000) 927–936.
[6] C.A. Fowler, F. Tian, H.M. Al-Hashimi, J.H. Prestegard, J. Mol. Biol. 304 (2000) 447–460.
[7] G.M. Clore, D.S. Garrett, J. Am. Chem. Soc. 121 (1999) 9008–9012.
[8] G.M. Clore, C.D. Schwieters, J. Am. Chem. Soc. 125 (2003) 2902–2912.
[9] M.R. Hansen, L. Mueller, A. Pardi, Nat. Struct. Biol. 5 (1998) 1065–1074.
[10] N. Tjandra, A. Bax, J. Magn. Reson. 124 (1997) 512–515.
[11] T.K. Hitchens, S.A. McCallum, G.S. Rule, J. Magn. Reson. 140 (1999) 281–284.
[12] D. Yang, J. Tolman, N.K. Goto, L.E. Kay, J. Biomol. NMR 12 (1998) 325–332.
[13] J.J. Chou, A. Bax, J. Am. Chem. Soc. 123 (2001) 3844–3845.
[14] N. Tjandra, A. Bax, J. Am. Chem. Soc. 119 (1997) 9576–9577.
[15] A. Bax, G. Kontaxis, N. Tjandra, Methods Enzymol. 339 (2001) 127–174.
[16] E.D. Alba, M. Suzuki, N. Tjandra, J. Biomol. NMR 19 (2001) 63–67.
[17] M. Ottiger, F. Delaglio, A. Bax, J. Magn. Reson. 131 (1998) 373–378.
[18] R.A. Venters, C. Huang, B.T. Farmer II, R. Trolard, L.D. Spicer, C.A. Fierke, J. Biomol. NMR 5 (1995) 339–344.
[19] B.K. Singleton, M.I. Torres-Arzayus, S.T. Rottinghaus, G.E. Taccioli, P.A. Jeggo, Mol. Cell Biol. 19 (1999) 3267–3277.
[20] F. Delaglio, S. Grzesiek, G.W. Vuister, G. Zhu, J. Pfeifer, A. Bax, J. Biomol. NMR 6 (1995) 277–293.
[21] A.J. Shaka, J. Keeler, R. Freeman, J. Magn. Reson. 52 (1983) 335–338.
[22] M. McCoy, L. Mueller, J. Am. Chem. Soc. 114 (1992) 2108–2110.
[23] L.E. Kay, P. Keifer, T. Saarinen, J. Am. Chem. Soc. 114 (1992) 10663–10665.
[24] D. Marion, M. Ikura, R. Tschudin, A. Bax, J. Magn. Reson. 85 (1989) 393–399.
[25] G. Zhu, A. Bax, J. Magn. Reson. 90 (1990) 405–410.